Original Article

MOLECULAR METABOLISM

ITCH E3 ubiquitin ligase downregulation compromises hepatic degradation of branched-chain amino acids

Rossella Menghini [1,19], Lesley Hoyles [2,19], Marina Cardellini [1,19], Viviana Casagrande [1], Arianna Marino [1], Paolo Gentileschi [3], Francesca Davato [1], Maria Mavilio [1], Ivan Arisi [4,5], Alessandro Mauriello [6], Manuela Montanaro [6], Manuel Scimeca [6], Richard H. Barton [7], Francesca Rappa [8,9], Francesco Cappello [8,9], Manlio Vinciguerra [10,11], José Maria Moreno-Navarrete [12], Wifredo Ricart [12], Ottavia Porzio [6], José-Manuel Fernández-Real [12,13], Rémy Burcelin [14], Marc-Emmanuel Dumas [7,15,16,17,], Massimo Federici [1,18,*]**

ABSTRACT

Objective: Metabolic syndrome, obesity, and steatosis are characterized by a range of dysregulations including defects in ubiquitin ligase tagging proteins for degradation. The identification of novel hepatic genes associated with fatty liver disease and metabolic dysregulation may be relevant to unravelling new mechanisms involved in liver disease progression

Methods: Through integrative analysis of liver transcriptomic and metabolomic obtained from obese subjects with steatosis, we identified itchy E ubiquitin protein ligase (*ITCH*) as a gene downregulated in human hepatic tissue in relation to steatosis grade. Wild-type or *ITCH* knockout mouse models of non-alcoholic fatty liver disease (NAFLD) and obesity-related hepatocellular carcinoma were analyzed to dissect the causal role of ITCH in steatosis

Results: We show that ITCH regulation of branched-chain amino acids (BCAAs) degradation enzymes is impaired in obese women with grade 3 compared with grade 0 steatosis, and that ITCH acts as a gatekeeper whose loss results in elevation of circulating BCAAs associated with hepatic steatosis. When *ITCH* expression was specifically restored in the liver of *ITCH* knockout mice, *ACADSB* mRNA and protein are restored, and BCAA levels are normalized both in liver and plasma

Conclusions: Our data support a novel functional role for ITCH in the hepatic regulation of BCAA metabolism and suggest that targeting ITCH in a liver-specific manner might help delay the progression of metabolic hepatic diseases and insulin resistance.

Keywords NAFLD; Metabolomics; Transcriptomics; BCAA

[1]Department of Systems Medicine, University of Rome "Tor Vergata", Via Montpellier 1, 00133, Rome, Italy [2]Department of Biosciences, Nottingham Trent University, Nottingham NG11 8NS, United Kingdom [3]Department of Surgery, University of Rome "Tor Vergata", Via Montpellier 1, 00133, Rome, Italy [4]European Brain Research Institute (EBRI) "Rita Levi-Montalcini", Viale Regina Elena, 295, 00161, Rome, Italy [5]CNR, Institute of Translational Pharmacology (IFT), Via del Fosso del Cavaliere 100, 00131, Rome, Italy [6]Department of Experimental Medicine, University of Rome "Tor Vergata", Via Montpellier 1, 00133, Rome, Italy [7]Imperial College London, Section of Biomolecular Medicine, Division of Systems Medicine, Department of Metabolism, Digestion and Reproduction, Imperial College London, Exhibition Road, London, SW7 2AZ, United Kingdom [8]Section of Human Anatomy, Department of Biomedicine, Neuroscience and Advanced Diagnostic (BIND), University of Palermo, Palermo, Italy [9]Euro-Mediterranean Institute of Science and Technology (IEMEST), Palermo, Italy [10]International Clinical Research Center (FNUSA-ICRC), St Anne University Hospital, Brno, Czech Republic [11]Institute of Liver and Digestive Health, Division of Medicine, University College London (UCL), London, United Kingdom [12]Department of Diabetes, Endocrinology and Nutrition, University Hospital of Girona 'Dr Josep Trueta' Institut d'Investigacio Biomedica de Girona IdibGi; and CIBER Fisiopatologia de la Obesidad y Nutricion, Girona, Spain [13]Department of Medical Sciences. School of Medicine, University of Girona, Spain [14]INSERM and University Paul Sabatier: Institut des Maladies Métaboliques et Cardiovasculaires, INSERM U1048 F-31432 Toulouse, France and Université Paul Sabatier, F-31432, Toulouse, France [15]Section of Genomic and Environmental Medicine, Respiratory Division, National Heart and Lung Institute, Imperial College London, Dovehouse St, London, SW3 6LY, United Kingdom [16]European Genomic Institute for Diabetes, CNRS UMR 8199, INSERM UMR 1283, Institut Pasteur de Lille, Lille University Hospital, University of Lille, 59045, Lille, France [17]McGill University and Genome Quebec Innovation Centre, 740 Doctor Penfield Avenue, Montréal, QC, H3A 0G1, Canada [18]Center for Atherosclerosis, University Hospital "Policlinico Tor Vergata", Italy

[19] These authors made equal contributions to this manuscript and share first authorship.

*Corresponding author. Department of Systems Medicine, University of Rome Tor Vergata, Via Montpellier 1, 00133, Rome, Italy. E-mail: federicm@uniroma2.it (M. Federici).

**Corresponding author. Imperial College London, Section of Biomolecular Medicine, Division of Systems Medicine, Department of Metabolism, Digestion and Reproduction, Imperial College London, Exhibition Road, London, SW7 2AZ, United Kingdom. E-mail: m.dumas@imperial.ac.uk (M.-E. Dumas).

Received September 9, 2021 • Revision received January 27, 2022 • Accepted January 28, 2022 • Available online 9 February 2022

https://doi.org/10.1016/j.molmet.2022.101454

Abbreviations

ITCH	itchy E ubiquitin protein ligase
NAFLD	non-alcoholic fatty liver disease
BCAAs	branched-chain amino acids
ACADSB	acyl-Coenzyme A dehydrogenase, short/branched chain
NASH	non-alcoholic steatohepatitis
HCC	hepatocellular carcinoma
MCD	methione–choline-deficient
DEN	di-ethyl-nitrosamine
TGF-β	transforming growth factor-beta
BMT	bone marrow transplantation
FABP4	fatty acid-binding protein 4
PRKKA2	Protein Kinase AMP-Activated Catalytic Subunit Alpha 2
SERPINE1	Serpin Family E Member 1
PDK4	pyruvate dehydrogenase kinase 4
IL-6ST	Interleukin 6 Cytokine Family Signal Transducer
LPL	lipoprotein lipase
TREM2	Triggering Receptor Expressed On Myeloid Cells 2
APOL3	apolipoprotein L3
SLAMF7	signaling lymphocytic activation molecule family member 7
IL4I1	Interleukin-4 Induced gene 1
EMILIN2	Elastin Microfibril Interfacer 2
COL1A1	Collagen Type I Alpha 1 Chain
ZNF683	zinc finger 683
LTB	Lymphotoxin beta
KCNN4	Potassium Calcium-Activated Channel Subfamily N Member 4
ALDH1B1	Aldehyde Dehydrogenase 1 Family Member B1
ALDH6A1	Aldehyde Dehydrogenase 6 Family Member A1
ALDH7A1	Aldehyde Dehydrogenase 7 Family Member A1
BCKDHB	Branched Chain Keto Acid Dehydrogenase E1 Subunit Beta
DBT	Dihydrolipoamide Branched Chain Transacylase E2
EHHADH	Enoyl-CoA Hydratase And 3-Hydroxyacyl CoA Dehydrogenase
HADHA	Hydroxyacyl-CoA Dehydrogenase Trifunctional Multienzyme Complex Subunit Alpha
MCCC2	Methylcrotonyl-CoA Carboxylase Subunit 2
ABAT	4-Aminobutyrate Aminotransferase
ACAA2	Acetyl-CoA Acyltransferase 2
ALDH9A1	Aldehyde Dehydrogenase 9 Family Member A1
AOX1	Aldehyde Oxidase 1
DLD	Dihydrolipoamide Dehydrogenase
GNMT	Glycine N-Methyltransferase
MAT1A	Methionine Adenosyltransferase 1A
PLIN2	Perilipin 2
SQSTM1	Sequestosome 1

1. INTRODUCTION

Obesity is associated with a constellation of disorders such as insulin resistance, dyslipidemia or hepatic steatosis. Non-alcoholic fatty liver disease (NAFLD) involves a series of liver abnormalities from simple hepatic steatosis to non-alcoholic steatohepatitis (NASH), which can ultimately lead to liver cirrhosis and cancer. Dysregulation of branched-chain amino acid (BCAA) metabolism has emerged as a key hallmark of these disorders, with converging experimental and epidemiological observations [1,2]. The BCAAs leucine, valine, and isoleucine are essential amino acids whose plasma concentrations are increased in metabolic diseases such as obesity and type 2 diabetes, are associated with the development of NAFLD, and strongly predict the risk of type 2 diabetes mellitus [3]. It is hypothesized that elevated circulating BCAAs observed in insulin resistance may result from dysregulated BCAA degradation [4]. In a diet-induced obesity mouse model, BCAA supplementation suppresses gluconeogenesis and activates lipogenesis, resulting in serious hepatic metabolic disorder and severe liver insulin resistance [5]. BCAAs play a key role as gatekeepers, feeding into upstream and downstream molecular pathways, and thus, they are major metabolic regulators involved in the pathophysiology of disease [6]. While insulin acutely increases BCAA oxidation in cardiac and skeletal muscle, chronically insulin-resistant mice show blunted BCAA oxidation in adipose tissues and liver, shifting BCAA oxidation toward muscle [7]. Targeting BCAA catabolism is a potential strategy to treat obesity-associated insulin resistance. In fact, experimental models have shown that restriction of dietary isoleucine led to reduced hepatic lipid deposition and smaller lipid droplets [8,9].

There is now accumulating evidence showing the E3 ubiquitin ligases—a large and diverse group of proteins with multiple binding domains to interact with ubiquitin, E2 enzymes, and substrate proteins—play a critical role in the tight regulation of metabolic and inflammatory processes in various contexts, including obesity [10–13]. Here, the analysis of liver transcriptomes and metabolomes from obese women with steatosis and data obtained from different mouse models of steatohepatitis and hepatocellular carcinoma (HCC) show a novel functional role for itchy E3 ubiquitin-protein ligase (ITCH) in the hepatic regulation of BCAA metabolism.

2. MATERIALS AND METHODS

2.1. Human studies

2.1.1. Human biopsies

ITCH immunochemistry was performed on samples from FLORINASH biobank [2] and stained with antibody Itch (ab31097, Abcam).

Formalin-fixed, paraffin-embedded biopsies were retrospectively collected from files of the Pathologic Anatomy Unit of the Civico Hospital, Palermo, Italy, and provided by M.V. and F.C. Briefly, 10 cases were selected of mild mixed macro- and micro-vesicular steatosis and 10 cases of HCC arising in macro-vesicular steatosis were also selected. The clinical characteristics of the patients studied were previously described [2] in terms of history of either HBV/HCV infection, cirrhosis, alcoholism, and NAFLD score. Fibrosis and/or cirrhosis were not observed in the biopsies. RNA was extracted from paraffinated slides using the RNeasy® FFPE Kit (QIAGEN) according to manufacturer instructions. Six subjects in the HCC groups and 6 subjects in the NAFLD group yielded enough RNA to perform ITCH qPCR.

All the procedures followed were in accordance with the ethical standards of the responsible committees (institutional and national) on human experimentation and with the Helsinki Declaration of 1975 (as revised in 2008). Written informed consent was obtained from all patients at the time of biopsy, and the study was approved by the Ethics Committee of the Civic Hospital, Palermo, Italy.

2.1.2. Transcriptomics data

A pilot microarray study was performed using Human Genome U133 Plus 2.0 Array (Affymetrix) (accession number GSE177050). Collection and processing of the FLORINASH expression data have been described previously [2]. The normalized data, available from ArrayExpress (accession E-MTAB-4856), were used in this study.

Microarray data were analyzed using R and the BioConductor package LIMMA (Linear Models for Microarray Data) [14], with the modifications for single channel data implemented [15]. An adjusted *P* value (false discovery rate) of less than 0.05 was used as a cut-off for identifying significantly differentially expressed genes (DEGs) [16]. Lists of DEGs, based on comparisons of *ITCH* low and high quartiles (1817 genes) and NAS 0 vs. NAS 3 (117 genes) were generated. Enrichr analysis was used to identify over-represented KEGG pathways and over-represented gene ontologies within the dataset [17,18].

2.1.3. Metabolic phenotyping of plasma by ^{1}H nuclear magnetic resonance (NMR) spectroscopy

Plasma samples were characterized as previously described [2]. Briefly, plasma samples were centrifuged at 12,000 g at 4 °C for 5 min, then 350 μL of sample was mixed with 150 μL of buffer before centrifugation at 12,000*g* at 4 °C for 5 min. Aliquots (600 μL) were transferred into a tube for automated acquisition on an NMR spectrometer (Bruker) operating at 600.22 MHz ^{1}H frequency as previously described [2]. The ^{1}H NMR spectra were pre-processed in MATLAB using in-house routines, including automatic phasing, baselining and referencing to the α-anomeric glucose doublet at 5.233 ppm; metabolic signals were recovered using statistical recoupling of variables. Metabolite identification and assignment were carried out using STOCSY, HMDB, BMRB and in-house databases. Multivariate modelling was performed using O-PLS-DA as previously reported [19,20].

2.2. Mouse models and intervention

2.2.1. Mouse model

ITCH knockout (*ITCH*$^{-/-}$) mice have been described previously [21]. Itch$^{+/-}$ female and male mice were crossed to generate Itch$^{+/+}$, Itch$^{+/-}$ and Itch$^{-/-}$ littermates. Genotyping was performed on tail biopsy DNAs by PCR. Itch$^{-/-}$ mice were born as expected by Mendelian ratio and are alive and fertile. Itch$^{-/-}$ mice and Itch$^{+/+}$ were used for experiments [22–24]. *ITCH*$^{-/-}$ mice and wild-type (WT) littermates on a C57Bl/6J background were maintained on 12-h light and dark cycles under controlled environmental conditions, with free access to water and food. Studies were performed only in male mice because gender may influence the severity of NASH in the MCD model. In fact, a comparison of the effects of an MCD diet between males and females revealed that the male gender showed the greatest degree of steatosis. Male C57/BL6 mice also showed the maximum lipid peroxidation, ultrastructural injury, inflammation and necrosis and showed more characteristics aligned with NASH [25,26]. In the NASH model, eight-week-old male C57Bl/6J or ITCH$^{-/-}$ mice were fed a normal diet (ND, standard chow 10% calories from fat; GLP Mucedola) and a methione–choline-deficient diet (MCD; 960,439, MP Biomedicals) for 4 (short-term) or 12 (long-term) weeks, as indicated. At the end of the treatments, blood samples were taken by retro-orbital bleeding with heparinized capillary tubes; next, the mice were euthanized, and the liver was excised rapidly to be used for further analysis. All specimens were stored at −80 °C.

For rescue experiments, 8-week-old male WT or ITCH$^{-/-}$ mice were injected retro-orbitally with PBS, 2,3 × 10^9 plaque-forming units (PFU) of ADV-GFP (Ad-CMV-GFP cat. no. 1768, Vectorbiolabs) or ADV-ITCH (Ad-GFP-mITCH cat. no. ADV-262418, Vectorbiolabs), once per week for 4 weeks, in combination with an MCD diet [27–30]. The obesity-hepatocellular carcinoma model induced by di-ethyl-nitrosamine (DEN) treatment was previously described [31]. Briefly, 25 mg/kg DEN was injected intraperitoneally into 14-day-old male mice. After 4 weeks, mice were fed a high-fat diet (HFD) until sacrifice at 36 weeks of age. Tumors were isolated and used for further analysis. Animal studies were performed from 2013 to 2014 and approved by the University of Tor Vergata Animal Care and Use Committee.

2.2.2. Metabolic tests

Blood glucose concentrations were determined using an automated Onetouch Lifescan Glucometer; Insulin and FFA levels in serum were measured using commercial kits (Insulin 10-1249-01, Mercodia; FFA MAK044, Sigma–Aldrich). Triglycerides extracted from liver tissues were analyzed using the Triglyceride Quantification Kit (ab65336, Abcam) according to the manufacturer's instruction. Briefly, ∼100 mg of tissue was washed with cold PBS, re-suspended and homogenised in 1 ml of 5% NP-40/ddH2O solution using a Dounce homogenizer. The samples were slowly heated to 95 °C in a water bath for 5 min, then cooled down to room temperature for two times to solubilize all triglycerides. After 2 min at top speed in a microcentrifuge to remove any insoluble material, samples were diluted 10-fold with ddH2O. Metabolic tests were performed in serum obtained from both fed conditions and after 6 h of fasting from WT and ITCH$^{-/-}$ mice, both before and/or after 4 weeks of an MCD diet.

2.2.3. Western blots

Western blots on total tissue lysates were performed as previously described [21]. The following antibodies were used: TGF-β (sc-7892, Santa Cruz), Actin (sc-47778, Santa Cruz), Tubulin (T9026, Sigma), ACADSB (ab129710, Abcam), Itch (ab31097, Abcam) and GFP (NB600-308, NOVUSBIO). For serum experiments, 5 μL of serum samples were subjected to SDS-PAGE and immunoblot analysis. The following antibodies were used: TNF alpha (ab6671, Abcam), MCP1 (ab7202-50, Abcam) and IL6 (AMC0864, Invitrogen).

2.2.4. Histochemical staining

The livers were fixed in 4% paraformaldehyde and embedded in paraffin, and the sections were then processed by hematoxylin and eosin (H&E) and Masson's Trichrome staining for histological evaluation of the NAFLD score [31]. For GFP staining, paraffin-embedded tissue was sliced into 3 μm sections, deparaffinized, and rehydrated with a decreasing gradient of alcohol. Antigen retrieval was performed in HIER solution at pH 6 and at 98 °C for 30 min. Sections were incubated for 1 h with anti-GFP (dilution 1:50, NB600-308, NOVUSBIO. Reactions were visualized by the UltraTek HRP Anti-Polyvalent Staining System (Scytek).

2.2.5. BCAA analysis

BCAA concentration in serum and liver tissue was determined using the Branched Chain Amino Acid Assay Kit (ab83374, Abcam), in accordance with the manufacturer's protocol. For tissue samples, 500 μl of the cold assay buffer were added to 10 mg of the liver. Using a Dounce homogenizer on ice, the tissues were lysed. Samples were spun down, and the supernatant was collected.

2.2.6. Gene expression analysis

Total RNA was isolated from liver using Trizol reagents (Invitrogen Corp., Eugene, OR). Total RNA (2 μg) was extracted and reverse-transcribed into cDNA using the High Capacity cDNA Archive kit (Applied Biosystems, Foster City, CA). A quantitative, real-time PCR was performed using an ABI PRISM 7700 System and TaqMan reagents (Applied Biosystems). Each reaction was performed in triplicate using standard reaction conditions, and the cycle threshold (Ct) value was normalized in mice by b-actin.

2.2.7. Bone marrow transplantation

Bone marrow transplantation (BMT) studies were performed as previously described [32]. Briefly, 8-week-old WT and *ITCH*$^{-/-}$ recipient mice were given busulfan (Sigma Aldrich) (20 mg/kg/day) and cyclophosphamide (Sigma Aldrich) (100 mg/kg/day). Mice were rested one day, and BMT was then performed. Bone marrow cells were harvested from WT and *ITCH*$^{-/-}$ mice femurs and tibias by flushing with PBS. After washing, bone marrow cells were injected in the retro-orbital venous plexus of the recipient mice. Feeding with an MCD diet began 4 weeks after engraftment. PCR for the *ITCH*$^{-/-}$ genotype was performed on DNA extracted from the blood of recipient mice 8 weeks after BMT to confirm the efficiency of this BMT technique.

2.3. Statistical analysis

Statistical data of the experimental studies were expressed as mean ± standard error of the mean (SEM). Statistical analyses were performed using GraphPad Prism (v.5.02). Groups were compared using a two-tailed unpaired Student's *t* test or one-way ANOVA with Bonferroni Multiple Comparison Test or Dunnett's Multiple Comparison Test, as indicated. Values of $p < 0.05$ were considered statistically significant.

3. RESULTS

3.1. Identification of novel targets for NAFLD in obese women

To identify novel targets in the development of metabolic-associated fatty liver disease (NAFLD), we performed a scoping transcriptome analysis comparing subjects with obesity, impaired glucose metabolism and steatosis >3 (n = 3 per group) to obese subjects with normal glucose tolerance and steatosis <1 (n = 3 per group) (Figure S1A). Several well-characterized markers of NAFLD were differentially expressed in the two groups; therefore, the expression levels of *FABP4*, *PRKKA2, SERPINE1* (significantly up-regulated), *PDK4*, and *IL-6ST* (significantly downregulated) (Figure S1B) were validated by qPCR. Interestingly, *ITCH* was among the most significantly down-regulated genes (Figures S1A and B). ITCH is an E3 ubiquitin ligase mostly known for its role in the regulation of inflammatory signals and auto-immunity [33,34], but its role(s) in hepatic steatosis remains undefined. To gain mechanistic insight on the role of *ITCH* in the NAFLD phenotype, we next investigated its expression in the FLORINASH hepatic whole-genome transcriptome database ($n = 88$, 32 men and 56 women) in relation to steatosis grade [2]. We confirmed that *ITCH* is among the 499 significantly differentially expressed genes (p-FDR < 0.05) when comparing steatosis degree (Steatosis 0 versus 3) in the whole FLORINASH liver transcriptome dataset (p-FDR = 0.019, mean expression 8.76, $\log_2$ fold change −0.30) (Table S1).

Immunohistochemical analysis of FLORINASH liver biopsies showed that ITCH protein abundance was negatively associated with steatosis (Figure 1A and Figure S2). We confirmed through linear models (adjusted for age, sex, and BMI) that low *ITCH* expression, assessed by qPCR, was significantly associated with ultrasound-assessed steatosis (Figure 1B) in the FLORINASH liver mRNA biobank ($n = 129$, clinical data are reported in Table S2). We also showed that *ITCH* was significantly downregulated when comparing NAFLD or NAFLD with signs of activity (inflammation and/or fibrosis) [35] in normal subjects (Figure 1C). Univariate analysis with post-hoc comparison of the clinical data for the whole cohort with available qPCR data ($n = 129$) showed that fasting insulin and HOMA-IR were significantly associated with *ITCH* expression, while the glucose disposal rate did not remain significant after correction for multiple testing (Table S3). Pearson and Spearman's rank-based correlation analysis showed that *ITCH* expression was associated with several markers of lipid and glucose metabolism and liver function (Table S3). We also found significantly reduced *ITCH* expression in RNA extracted from liver biopsies from subjects with obesity/NAFLD-related hepatocellular carcinoma compared with those with NAFLD ($n = 6$ per group, $p < 0.05$) (Figure 1D) [36]. These results suggest that *ITCH* expression is consistently downregulated in multiple liver disease contexts.

3.2. Transcriptomics signatures between low ITCH expression and grade 3 steatosis

We next stratified the female subjects ($n = 56$) with available transcriptomic data according to *ITCH* quartiles. Comparison of Quantile 1 (L, ITCH^{low}) and Quantile 4 (H, ITCH^{high}) by LIMMA analysis revealed 1,817 genes that were significantly differentially expressed between the two groups (adj. P value < 0.05) (Figure 1E and Table S4). We then analyzed the same group after stratification for steatosis (grade 3 (steatosis^{high})) compared with steatosis grade 0) and found 117 genes to be significantly (adj. P value < 0.05) differentially expressed between the two steatotic groups (Table S5).

The overlap between steatosis^{high}- and ITCH^{low}-associated genes identified 92 intersecting significantly differentially expressed genes (Figure 1F and Table S6). The 10 top upregulated genes common to ITCH^{low} and steatosis^{high} were *LPL*, *TREM2*, *APOL3*, *SLAMF7*, *IL4I1*, *EMILIN2*, *COL1A1*, *ZNF683*, *LTB* and *KCNN4*, which are involved in inflammation and fibrosis (Table S6). Among the top down-regulated genes common to ITCH^{low} and steatosis^{high}, we found genes involved in BCAA degradation (Figure 1G and Table S6).

Next, we performed an enrichment analysis of the 92 intersecting genes and found that the most significant represented pathway was 'valine, leucine and isoleucine degradation' (Figure S3 and Table S7). Among the 1,817 genes associated with ITCH^{low} (adj. P value < 0.05), 10 (*ACADSB*, *ALDH1B1*, *ALDH6A1, ALDH7A1*, *BCKDHB*, *DBT*, *EHHADH*, *HADHA*, *IL4I1*, and *MCCC2*) belonged to the human KEGG pathway 'Valine, leucine, and isoleucine degradation'. When the adjusted P threshold was increased to 0.1 (2,765 significantly differentially expressed genes), five additional genes (*ABAT*, *ACAA2*, *ALDH9A1*, *AOX1*, and *DLD*) belonging to the pathway were significantly differentially expressed (Figure 2 and Table S4).

We then analyzed plasma metabolites profiled by ^{1}H NMR spectroscopy and built multivariate O-PLS analyses to integrate functional datasets of steatosis with *ITCH* qPCR data. Remarkably, the steatosis and *ITCH* metabolic signatures depicted in the O-PLS model coefficient plots presented reciprocal inverse patterns suggestive of mirrored metabolic signatures for blood plasma metabolites (Figure 3A,B). Using permutation testing with 10,000 iterations, we confirmed the opposite trends between *ITCH* and steatosis for ^{1}H NMR resonances corresponding to $-CH_3$ and $-CH_2$- from lipoproteins, lactate, glucose and BCAAs. These results showed that the low *ITCH* expression quartile and the steatosis 3 group had similar metabolic profiles, which strengthens the possible involvement of the downregulation of *ITCH* in the pathogenesis of NAFLD.

ITCH expression (qPCR data) for 78 women showed a significant negative correlation (adj. P value < 0.1) with valine and isoleucine levels in plasma (Table S8). Altogether, these transcriptomic and metabolic results suggest that when *ITCH* expression is low, degradation of BCAAs decreases because of downregulation of genes within the degradation pathway, leading to increased abundance of these metabolites in plasma.

In summary, our clinical studies showed that lower *ITCH* hepatic expression in obese subjects is associated with NAFLD, with evidence of dysregulation at hepatic gene expression and metabolic levels.

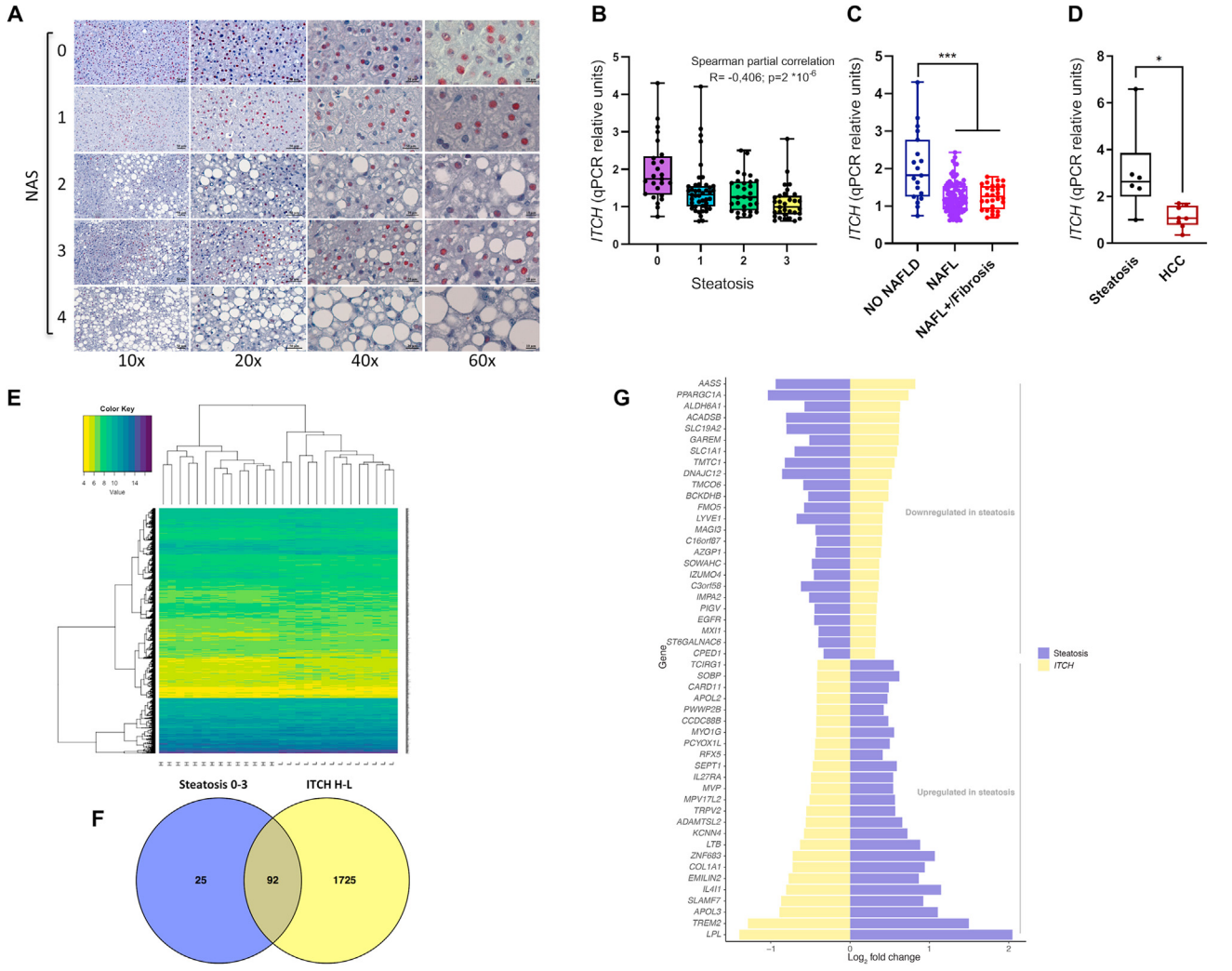

Figure 1: *ITCH* expression is in the hepatocyte and kupffer cell fraction and reduced in steatotic areas. A) Immunohistochemical studies revealed that *ITCH* expression was reduced specifically in steatotic regions. **B)** *ITCH* expression decreases as steatosis score increases ($n = 129$, Spearman partial correlation $p < 2 \times 10^{-6}$ after correction for age, BMI and country). **C)** *ITCH* expression in subjects with different NAFLD characteristics (n = 129, ***$p < 0.001$ with One-way Anova and Kruskall–Wallis test). **D)** *ITCH* expression in HCC and NAFLD patients ($n = 6$ per group; Student's *t* test *$p < 0.05$). **E)** Heat map showing the 1,817 genes differentially expressed when comparing the data based on lower (lo) and higher (hi) *ITCH* quantiles ($n = 56$ females). Data were $\log_2$-transformed and scaled to produce the heat map. **F)** Number of significantly differentially expressed genes that intersect based on analyses of genes by *ITCH* and steatosis. Differential gene expression was determined for the lowest and highest *ITCH* quartiles and for data based on steatosis 0 vs steatosis 3. **G)** Top 25 upregulated and downregulated genes when comparing intersecting genes in the context of *ITCH* expression and steatosis.

3.3. Evidence for ITCH and BCAA interplay in experimental models

To dissect the causal role of ITCH in steatosis, we turned to animal models. First, we used short-term (4 weeks) and long-term (12 weeks) methione–choline-deficient (MCD) diets to mimic the initial and late stages of steatohepatitis (Figure 4A), as confirmed by downregulation of *GNMT* and *MAT1A* and increased *COL1A1* as in non-alcoholic steatohepatitis (NASH) (Figure S4A) [37]. We observed that intrahepatic BCAAs were upregulated in mice treated for 12 weeks with the MCD (Figure 4A), with concomitant downregulation of *ITCH*, *ACADSB*, and *ALDH6A1* and other BCAA degradation-associated genes (*BCKDHB*, *EHHADH*, *ACCA2*, *ABAT*, and *AOX1*); we found that expression of BCAT2 remained unaffected by diet (Figure 4B and Figure S4B). Next, because obesity is a bona fide promoter of liver cancer [38], and to understand whether ITCH plays a role in the continuum between steatohepatitis and its complications such as HCC, we analyzed an established model of HCC that combines dietary and genetic risk (Figure S4C) [30]. Treatment with di-ethyl-nitrosamine (DEN) at 14 days only induced hepatic nodules at 8 months (32 weeks later), while the combination of DEN treatment with the HFD feeding from 8 weeks of age induced a fully blown HCC phenotype at 8 months (Figure S4D). *ITCH* expression decreased in HCC from mice treated with DEN + HFD. In the HFD-HCC model, like in the MCD model, genes involved in steatohepatitis were consistently downregulated (*GNMT*, *MAT1A*) or up-regulated (*COL1A1*) (Figure S4E). Consistent with our human data and MCD model, the downregulation of BCAA degradation genes (*ABAT*, *ACAA2*, *ACADSB*, *ALDH6A1*, and *BCKDHB*) mirrored ITCH downregulation in the HCC model (Figure S4E).

3.4. Modulation of ITCH in vivo modifies BCAA levels

Having established that *ITCH* is a gene related to the progression of NAFLD, we then used the whole-body *ITCH* knockout ($ITCH^{-/-}$) fed a short-term (4 weeks) MCD diet as a model of liver lipotoxicity; we found that *ITCH* deletion promotes steatohepatitis (Figure 4C and Figure S5), increased expression of a fibrosis mediator such as TGF-β (Figure 4D) and reduced expression of *ACADSB* (Figure 4E). Despite the

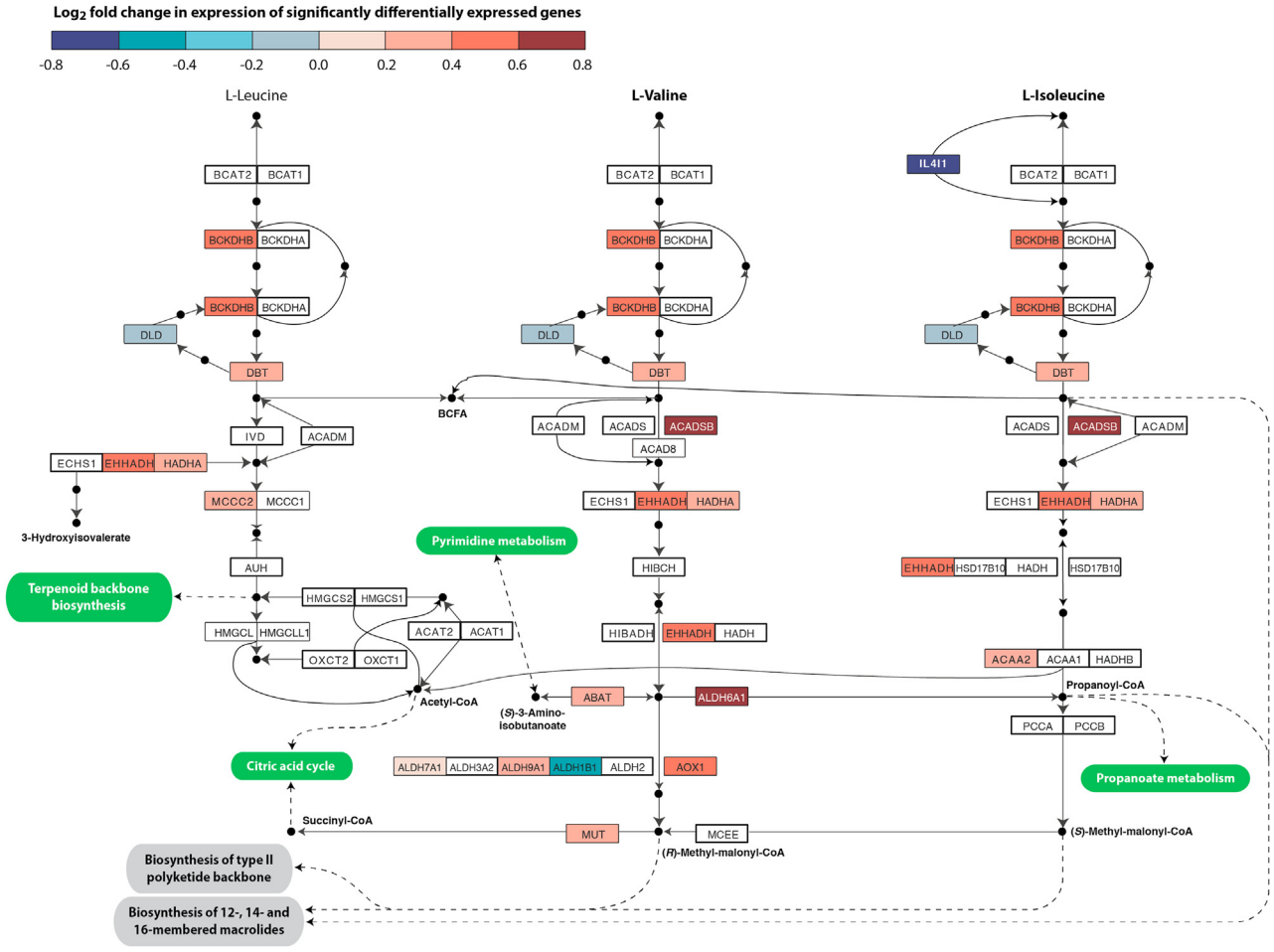

Figure 2: Integration of *ITCH* qPCR data, plasma metabolite data and *ITCH*-associated differentially expressed genes. Among the 2,765 genes found to be significantly (adjusted p value < 0.1) differentially expressed when analyses were based on low or high *ITCH* expression, 15 belonged to the human KEGG pathway 'Valine, Leucine, and Isoleucine degradation'. Black dots represent metabolic intermediates in the pathway. Only end-point metabolites are annotated. Pathways shown in green boxes also contain genes that are significantly differentially expressed when microarray data are analyzed based on *ITCH* quartiles. White box around gene name, gene not significantly differentially expressed; colored box around gene name, log_2-fold change (refer to color scale in figure).

significant weight reduction in $ITCH^{-/-}$ mice compared to WT, metabolic parameters like glucose, insulin and FFA serum levels, assessed before and after 4 weeks of an MCD diet, and triglyceride levels in liver showed no relevant differences between WT and $ITCH^{-/-}$ mice. This suggests that loss of ITCH primarily impacts the NAFLD phenotype rather than being a secondary result of metabolic derangements (Table S9). We then implemented a rescue strategy using adenovirus encoding *ITCH* (ADV-ITCH) in both WT and $ITCH^{-/-}$ mice fed a short-term MCD diet (Figure 5A). After 4 weeks of weekly injections of ADV-ITCH, we found that the weight of ITCH−/− was lower than WT, with a trend to increase in ITCH−/− injected with ADV-ITCH (Figure S6A). On the contrary, ITCH−/− showed a mild but not significant increase in triglycerides, which tended to decrease after the ADV-ITCH injection (Figure S6B). Immunohistochemical analysis showed that GFP was expressed in mice injected with ADV-GFP and ADV-ITCH, both in hepatocytes (asterisk) and kupffer cells (arrow) (Figure S6B and Figure S7A). GFP protein expression was confirmed by western blot in liver (Figure S7B).

ITCH expression was significantly increased in liver from *ITCH*−/− mice that were fed a short-term MCD, compared to control and ADV-GFP injected mice (Figure 5B), but resulted undetectable in other tissues, such as muscle and spleen (Figure S8A). Consistent with clinical observation that low ITCH expression reduces hepatic BCAA catabolism, we found increased BCAA levels in serum and liver from $ITCH^{-/-}$ mice compared with WT fed a short-term MCD, but we found normalization of BCAA levels in $ITCH^{-/-}$ liver when *ITCH* expression was rescued (Figure 5C). ACADSB mRNA and protein levels behave accordingly (Figure 5D). Expression of inflammatory markers (TNF alpha, MCP1 and IL6) in serum increased in $ITCH^{-/-}$ mice as compared that in WT, which showed a blunted reduction after adenoviral treatment (Figure S8B).

Given the inflammatory component triggered by *ITCH* [39], we assessed whether the *ITCH*-induced steatohepatitis phenotype is a consequence of the *ITCH*-induced inflammatory phenotype in immune cells, thus proceeding to BMT between WT and $ITCH^{-/-}$ mice fed a short-term MCD (Figure S9A). We observed a gradual increase in steatohepatitis score by comparing WT → WT, $ITCH^{-/-}$ → WT, WT → $ITCH^{-/-}$, and $ITCH^{-/-}$ → $ITCH^{-/-}$ (Figure S9B), which suggests that *ITCH* expression in both hepatic and myeloid cells plays a role in the NASH phenotype (Figure S9, Table S10). ACADSB mRNA and protein levels (Figure 5E), but not triglycerides (Figure S9C), followed the same pattern.

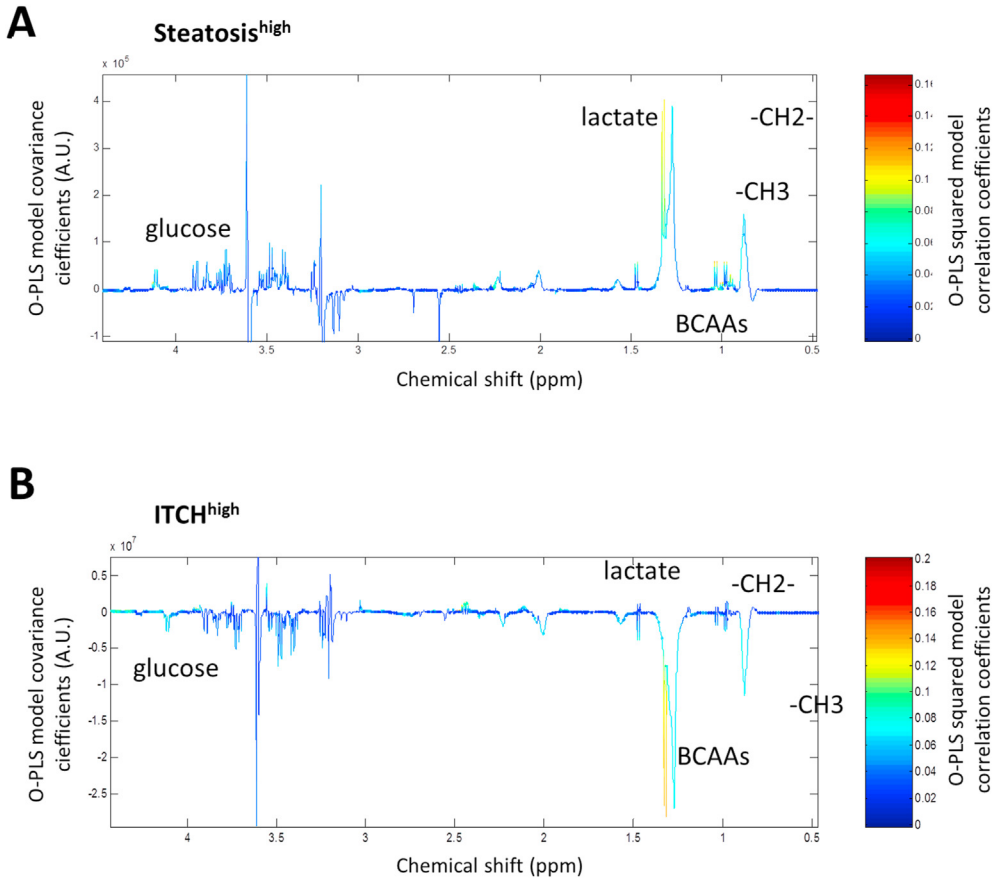

Figure 3: Plasma metabolites profiled by ^{1}H NMR spectroscopy and multivariate O-PLS analyses integrating functional datasets steatosis and *ITCH* qPCR data. A) Model coefficient plot for an O-PLS regression model using ^{1}H NMR metabolic profiles to fit NAS, represented in a pseudo-spectrum plot according to the ^{1}H NMR chemical shift, in which the line shape is derived from mean-centered model coefficients related to covariance whilst the color-scale is derived from unit-variance model coefficients related to correlation. **B)** Model coefficient plot for an O-PLS regression model using ^{1}H NMR metabolic profiles to fit ITCH quartiles, represented in a pseudo-spectrum plot according to the ^{1}H NMR chemical shift.

4. DISCUSSION

In recent years, the use of metabolomics and lipidomics, alongside integration with transcriptomics data, has prompted identification of targets to further explore for treatment in, or prevention of, human NAFLD [40–43]. A two-stage metabolic and molecular screening of liver tissue showed that hydroquinone and nicotinic acid were inversely correlated with histological NAFLD severity [44]. Another study that profiled changes in hepatic BCAA metabolite levels, with transcriptomic changes in the progression of human NAFLD, outlined that the transition from steatosis to NASH was associated with increases in levels of leucine, isoleucine, and valine (147%), as well as with significant downregulation of amino acid and BCAA metabolism gene sets [45]. A strong association of obesity and insulin resistance with increased circulating levels of branched-chain levels has for decades been recognized in human subjects [46].

The interplay of BCAAs metabolism with metabolic health is therefore a translatable option for the treatment of obesity and insulin resistance; however, further investigation is warranted to better understand the molecular basis.

Here we added one potential partner in the still fragmentary molecular scenario underlying the role of BCAAs in metabolic health. Altogether, with clinical studies and animal models, we demonstrate that the downregulation of *ITCH* affects the hepatic transcriptome and plasma metabolome (BCAAs and glucose homeostasis) in a coordinated manner, with implications for increased risk of developing steatosis to NASH and HCC. This is a novel functional role for ITCH, which is a ubiquitin ligase typically tagging proteins for proteasome degradation to regulate immune functions in autoimmune disease, autophagy, and cancer [33,34,47,48].

Interestingly, we found that isoleucine and valine, but not leucine, were inversely correlated with the hepatic expression of ITCH. Dietary levels of isoleucine are positively associated with BMI in humans. Furthermore, two studies independently proved that in obese mice, the lowering of BCAA circulating levels by a decrease in consumption of BCAA in the diet, particularly isoleucine and valine, promoted metabolic health and rapid fat mass loss even without calorie restriction [8,9]. Another study found that short-term dietary reduction of BCAAs decreases postprandial insulin secretion and improves white adipose tissue metabolism and gut microbiome composition in patients with type 2 diabetes [49]. In Zucker-fatty rats, branched-chain amino acid restriction improves muscle insulin sensitivity by enhancing efficiency of fatty acid oxidation and acyl-glycine export [50], while others did not observe any effect of BCAA supplementation on glucose homeostasis in mice [51,52]. Overall, further studies are needed to definitively prove a potential metabolic benefit from the reduction of BCAA.

Our data have clear clinical relevance as we have identified a gene at the intersection of several pathways involved in the benign steatosis to

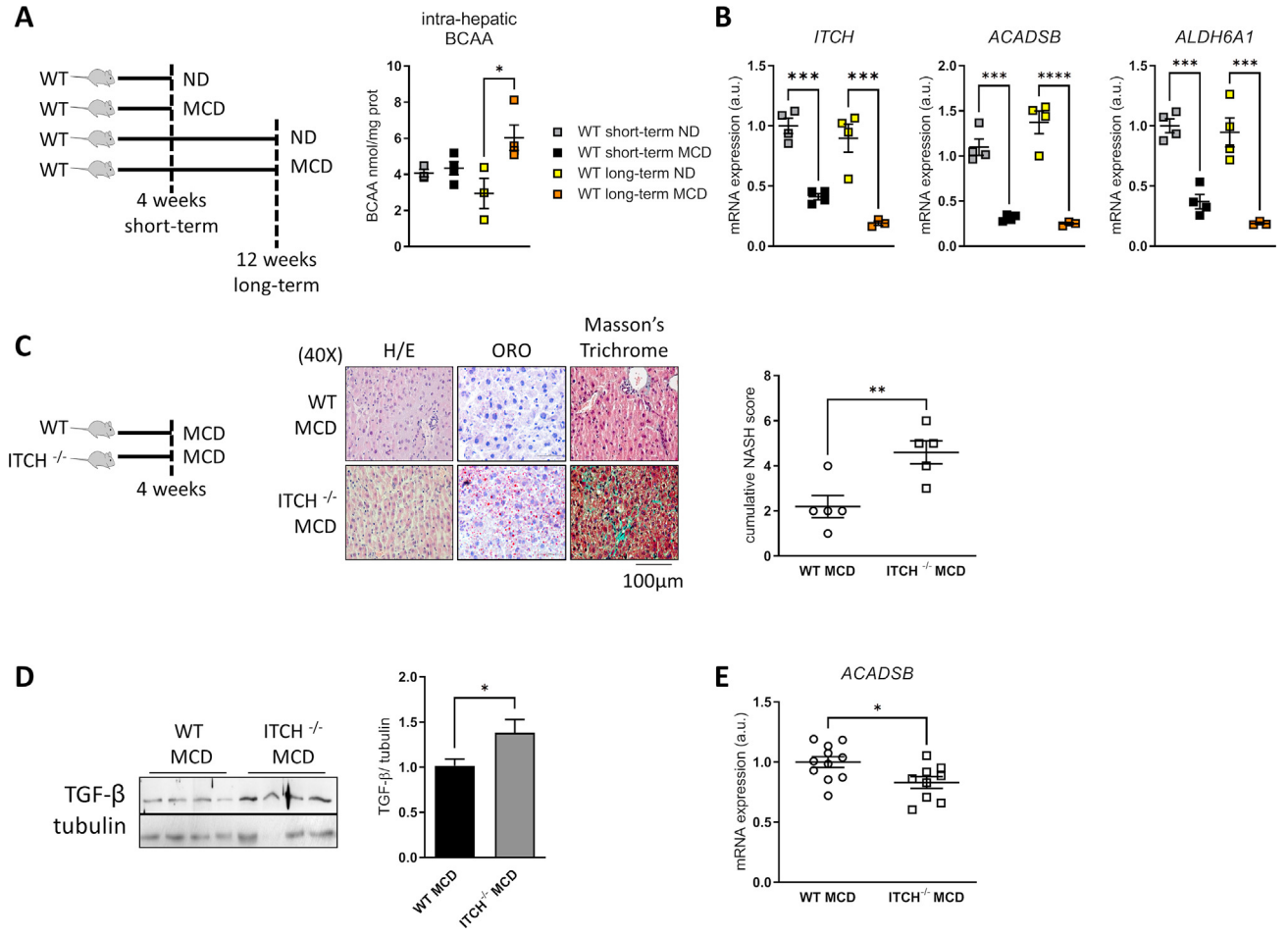

Figure 4: Effect of MCD on wild type (WT) and ITCH knockout (*ITCH*$^{-/-}$) mice. A) Intra-hepatic BCAAs are increased and **B)** *ITCH*, *ACADSB* and *ALDH6A1* mRNA expression are reduced in liver from WT mice fed MCD compared with WT mice fed ND for 12 weeks (n = 3–4 per group; *p < 0.05, ***p ≤ 0.001, ****p ≤ 0.0001; one-way ANOVA with Bonferroni Multiple Comparison Test, data are means ± SEM); **(C and D)** After 4 weeks of MCD diet, *ITCH*$^{-/-}$ showed increased steatosis and fibrosis compared with WT. Steatosis, inflammatory activity and fibrosis cumulatively determined a higher NASH score and increased TGFβ in *ITCH*$^{-/-}$ fed short-term MCD diet compared with WT fed short-term MCD diet (n = 5 per group). **E)** Decreased *ACADSB* mRNA expression in *ITCH*$^{-/-}$ MCD compared with WT MCD (n = 11–9 per group; *p < 0.05, **p ≤ 0.01; Student's t-test, data are mean ± SEM).

deleterious steatohepatitis transition. In particular, lower hepatic *ITCH* expression in human subjects is associated with two factors—that is, apoptosis and regulation of cellular response to stress—believed to be involved in the NAFLD to NASH transition [53].

In human pathology, mutations in the *ITCH* gene (located on chromosome 20q11.22) can lead to a deficiency of the encoded protein and increased T cell activity with manifestation of a complex, systemic autoimmune disease, including hepatic failure [54,55]. Our study did not include subjects with autoimmune disease, but analysis of Gene Ontology of *ITCH*-associated pathways highlighted cytokine signaling, neutrophil functions, and T cell activation, suggesting that ITCH is also a regulator of immune and inflammatory pathways in hepatic metabolic disorders.

The role of BCAA catabolism in NAFLD remains unclear. We previously showed that primary human hepatocytes use BCAAs as a primary substrate, especially under free fatty acid and phenyl acetic acid treatment [2]. Here, we also observed a mild BCAT2 expression in liver. Other studies have shown that the transition from normal liver to NAFLD stages is associated with adaptive downregulation of several genes involved in BCAA catabolism, including BCKDHA complex [45].

The effect of ITCH on BCAA catabolism may help explain recent observations in mice in which obesity and insulin resistance redistribute whole-body BCAA oxidation. In fact, in healthy conditions, oxidation in adipose tissue and the liver prevents excessive shunt of BCAAs to the muscle. Suppression of BCAA oxidation in liver and adipose tissues promotes elevations in plasma BCAAs, likely shunting BCAA oxidation to permissive organs. Consistent with these observations, recent studies in whole animals with steady-state, heavy isotope infusions revealed in db/db mice blunted BCAA oxidation in fat and liver, with consequent significant shunting of oxidation to skeletal muscle [56,57]. However, in our reconstitution experiment, we observed that the adenovirus encoding for ITCH also affected liver macrophages. Interestingly, reduced BCAA catabolism is observed in macrophages from db/db mice, and enhancing BCAA catabolism with pharmacological activator attenuates inflammation and tissue fibrosis in liver [58]. Similarly, it has been shown that BCAT1 controls metabolic reprogramming in activated human macrophages and is associated with inflammatory diseases [59]. Therefore, we cannot exclude that the effect of ITCH on BCAA catabolism is determined in the myeloid rather than the hepatic compartment.

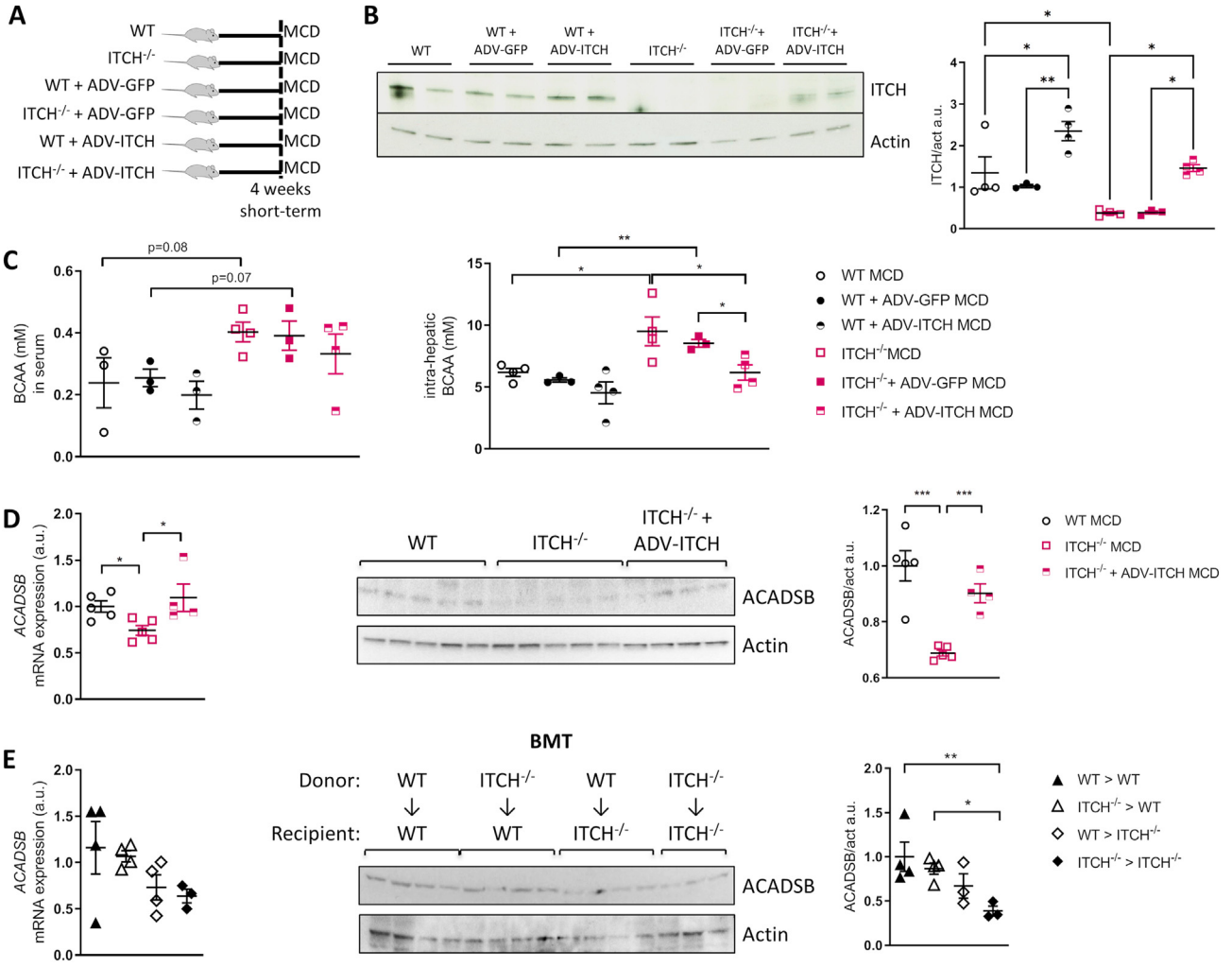

Figure 5: Modulation of BCAAs in ITCH$^{-/-}$ MCD. A) WT or *ITCH*$^{-/-}$ mice were injected retro-orbitally with PBS, ADV-GFP or ADV-ITCH once a week for 4 weeks, in combination with MCD diet. **B)** Protein expression of ITCH in liver is increased in ITCH$^{-/-}$ MCD after treatment with ADV-ITCH. (n = 3–4 per group). A representative image of 2 mice per group is shown. **C)** Circulating BCAAs are increased in *ITCH*$^{-/-}$ compared with WT on or MCD (p = 0,08, n = 3–4 per group); intra-hepatic BCAAs are increased in *ITCH*$^{-/-}$ MCD compared with WT MCD and decreased after treatment with ADV-ITCH (n = 4 per group); **C)** ACADSB mRNA and protein are decreased in *ITCH*$^{-/-}$ MCD compared with WT MCD (n = 5 per group) and increased after treatment with ADV-ITCH (n = 4 per group); **D)** ACADSB mRNA and protein in bone marrow transplant (BMT) model are significantly reduced in *ITCH*$^{-/-}$ transplanted with ITCH$^{-/-}$ bone marrow compared to WT transplanted either with WT- or *ITCH*$^{-/-}$- bone marrow (n = 3–4 per group). (*p < 0.05, **p ≤ 0.01, ***p ≤ 0.001; Student's *t* test, data are mean ± SEM).

Our study has limitations. First, our results clearly demonstrate that modulating ITCH expression in the hepatic tissue by re-expressing it in the hepatocytes via the adenovirus approach or in the non-hepatic compartment via bone marrow transplantation, results in parallel modulation of BCAA levels and ACADSB mRNA and protein levels in the liver. However, loss of ITCH is expected to reduce protein degradation, suggesting that ITCH targets one or more proteins acting as a co-repressor for BCAA catabolic gene expression. Identification of these targets will require a proteomics-based approach to be performed in future works.

Second, the effect of ITCH on hepatic steatosis may not be restricted to the regulation of BCAA. In fact, it has been shown that ITCH may affect the lipid droplet binding protein Perilipin 2 degradation [60]. Ablation of perilipin 2 (PLIN2), the most abundant lipid droplet-associated protein in steatotic liver, protects mice from diet-induced NAFLD [61]. Reduced ITCH expression increases Perilipin 2 on lipid droplets, which in turn increases lipid droplets formation in hepatocytes [62,63]. In humans, high levels of Plin2 are present in sarcopenia, hepatic steatosis, atherosclerosis and some types of cancer [64]. ITCH polyubiquitinates PLIN2 (and potentially other lipid droplets-associated proteins), leading to the association of the macroautophagy cargo receptor SQSTM1/p62, which triggers macrolipophagy [65]. It has been hypothesized that ITCH-mediated ubiquitination of PLIN2 could initiate Ub-dependent macrolipophagy, but more direct evidence supporting this notion needs to be collected [66]. Effects of ITCH on PLIN2 might also help explain the slight difference between liver ORO staining (increased) and triglyceride levels (which only tend to increase) in response to diminished ITCH expression. In fact, ORO also stains neutral lipids such as cholesterol and diacylglycerol, and PLIN2 is known to facilitate the storage of neutral lipids within lipid droplets. However, further studies across more specific models are needed to understand the role of ITCH E3-mediated degradation of PLIN2 in cardiometabolic disorders and the link between neutral lipids content in lipid droplets.

We used mouse models to confirm the link between ITCH and BCAA degradation found in human analysis; however, mice models do not

perfectly match human NAFLD. In particular, the whole-body ITCH knockout has different phenotypes, due to pleiotropic effects of ITCH on inflammation and autoimmunity, that may imply actions on different targets [39]. From our human and mouse models, we observed the loss of ITCH expression in both hepatocyte and non-hepatocyte compartments, but whether one or both is more relevant in the context of NAFLD remains unclear. Finally, NAFLD is often linked to dysfunctional adipose tissue. Since we previously found that global loss of ITCH may exert a TH2/M2 reaction in WAT and atherosclerotic plaque in mice, it will be necessary to understand in human subjects whether the reduction of ITCH is part of an adaptive response to an increase in oxidative pathways [21,32]. Intriguingly, beside the role of ITCH E3 ligase in the Ub pathway, the reduction of ITCH is mirrored by a reduction in circular ribonucleic acid (circRNA) ITCH [67,68]. Recent reports have suggested that a reduction of circ-ITCH may have implications in carcinogenesis including effects on hepatocellular carcinoma [69–72].

In conclusion, our human and mouse data suggest that increased circulating BCAA levels, a hallmark of metabolic and cardiovascular diseases, may be partly mediated by loss of ITCH regulation of BCAA degradation enzymes in the liver cells. Beyond NAFLD, given the prevalence of BCAA dysregulation in obesity, this work highlights ITCH as an actionable candidate to normalize BCAA metabolism in obesity and more generally in cardiometabolic disorders.

GRANT SUPPORT

This work was in part supported by EU-FP7 FLORINASH (Health-F2-2009-241,913), Fondazione Roma NCD 2015 grant, PRIN 2015MPESJS, PRIN 2017FM74HK, ARS01_00876 BIO-D and IMI2 SOPHIA (to M.F.), by the NIHR Imperial Biomedical Research Centre and by grants from the French National Research Agency (ANR-10-LABX-46 [European Genomics Institute for Diabetes]), from the National Center for Precision Diabetic Medicine [PreciDIAB], which is jointly supported by the French National Agency for Research (ANR-18-IBHU-0001), by the European Union (FEDER), from the Hauts-de-France Regional Council and from the European Metropolis of Lille (MEL) and from Isite ULNE, also jointly funded by ANR (ANR-16-IDEX-0004-ULNE) the Hauts-de-France Regional Council and by the European Metropolis of Lille (MEL), from Fondo Europeo de Desarrollo Regional (FEDER) through the Programa Interreg V-A España-Francia- Andorra (POCTEFA 2014–2020), from FIS project from the Instituto de Salud Carlos III PI18/01022, from Fondo Ordinario Enti (FOE D.M 865/2019), agreement Italian National Research Council – EBRI (2019–2021) (I.A.). This work used the computing resources of the UK MEDical BIOinformatics partnership—aggregation, integration and visualisation—and analysis of large, complex data (UK MED-BIO), which was supported by the Medical Research Council (grant number MR/L01632X/1). L.H. was an MRC Intermediate Research Fellow in Data Science, funded by the UK MEDical BIOinformatics partnership (UK Med-Bio, grant number MR/L01632X/1); M.V. is funded by European Regional Development Fund-Project MAGNET (No. CZ.02.1.01/0.0/0.0/15_003/0000492).

DATA AVAILABILITY STATEMENT

All microarray data associated with the FLORINASH study are available from ArrayExpress under accession E-MTAB-4856 at https://www.ebi.ac.uk/arrayexpress/experiments/E-MTAB-4856/

AUTHOR CONTRIBUTIONS

Planning and concept of study: R.B., E.H., J.K.N., J.M.F.R., M.F. Acquisition of data: R.M., L.H., M.C., V.C., A.Mar., P.G., F.D., M.M., A.Mau., R.H.B., F.R., F.C., M.V., J.M.M.N., W.R., O.P. Statistical analysis: L.H., M.C., R.M., V.C. Data interpretation and manuscript revision: R.M., L.H., R.B., J.M.F.R., M.D., M.F. Writing committee: R.M., L.H., R.B., J.M.F.R., M.E.D., M.F. Manuscript preparation: R.M., M.C., L.H., R.B., J.M.F.R., M.E.D., M.F. L.H. carried out all transcriptomic analyses associated with the FLORINASH dataset. All authors contributed to the analyses and interpretation of data and to the writing of the manuscript.

ETHICS APPROVAL

All subjects gave written informed consent, validated and approved by the ethical committee of the Hospital Universitari Dr Josep Trueta (Comitè d'Ètica d'Investigació Clínica, approval number 2009 046) and Policlinico Tor Vergata University of Rome (Comitato Etico Indipendente, approval number 28-05-2009). Animal procedures were approved by local and national committees in charge (Tor Vergata University Institutional Animal Care and Use Committee and Ministry of Health, license no. 438/2019-PR) and conducted in accordance with accepted standards of humane animal care.

CONFLICT OF INTEREST

None declared.

APPENDIX A. SUPPLEMENTARY DATA

Supplementary data to this article can be found online at https://doi.org/10.1016/j.molmet.2022.101454.

REFERENCES

[1] Newgard, C.B., An, J., Bain, J.R., Muehlbauer, M.J., Stevens, R.D., Lien, L.F., et al., 2009. A branched-chain amino acid-related metabolic signature that differentiates obese and lean humans and contributes to insulin resistance. Cell Metabolism 9(4):311–326.

[2] Hoyles, L., Fernández-Real, J.M., Federici, M., Serino, M., Abbott, J., Charpentier, J., et al., 2018. Molecular phenomics and metagenomics of hepatic steatosis in non-diabetic obese women. Natura Med 24(7):1070–1080.

[3] Jang, C., Oh, S.F., Wada, S., Rowe, G.C., Liu, L., Chan, M.C., et al., 2016. A branched-chain amino acid metabolite drives vascular fatty acid transport and causes insulin resistance. Natura Med 22(4):421–426.

[4] Gannon, N.P., Schnuck, J.K., Vaughan, R.A., 2018. BCAA metabolism and insulin sensitivity - dysregulated by metabolic status? Molecular Nutrition & Food Research 62(6):e1700756.

[5] Zhao, H., Zhang, F., Sun, D., Wang, X., Zhang, X., Zhang, J., et al., 2020. Branched-chain amino acids exacerbate obesity-related hepatic glucose and lipid metabolic disorders via attenuating Akt2 signaling. Diabetes 69(6):1164–1177.

[6] Zhang, Z.Y., Monleon, D., Verhamme, P., Staessen, J.A., 2018. Branched-chain amino acids as critical switches in health and disease. Hypertension 72(5):1012–1022.

[7] Neinast, M.D., Jang, C., Hui, S., Murashige, D.S., Chu, Q., Morscher, R.J., et al., 2019. Quantitative analysis of the whole-body metabolic fate of branched-chain amino acids. Cell Metabolism 29(2):417–429 e4.

[8] Cummings, N.E., Williams, E.M., Kasza, I., Konon, E.N., Schaid, M.D., Schmidt, B.A., et al., 2018. Restoration of metabolic health by decreased consumption of branched-chain amino acids. Journal of Physiology 596(4):623–645.

[9] Yu, D., Richardson, N.E., Green, C.L., Spicer, A.B., Murphy, M.E., Flores, V., et al., 2021. The adverse metabolic effects of branched-chain amino acids are mediated by isoleucine and valine. Cell Metabolism 33(5):905–922.e6.

[10] Zhang, T., Kho, D.H., Wang, Y., Harazono, Y., Nakajima, K., Xie, Y., et al., 2015. Gp78, an E3 ubiquitin ligase acts as a gatekeeper suppressing nonalcoholic steatohepatitis (NASH) and liver cancer. PLoS One 10(3):e0118448.

[11] Yamada, T., Murata, D., Adachi, Y., Itoh, K., Kameoka, S., Igarashi, A., et al., 2018. Mitochondrial stasis reveals p62-mediated ubiquitination in parkin-independent mitophagy and mitigates nonalcoholic fatty liver disease. Cell Metabolism 28(4):588–604 e5.

[12] Lee, M.S., Han, H.J., Han, S.Y., Kim, I.Y., Chae, S., Lee, C.S., et al., 2018. Loss of the E3 ubiquitin ligase MKRN1 represses diet-induced metabolic syndrome through AMPK activation. Nature Communications 9(1):3404.

[13] Zhu, K., Tang, Y., Xu, X., Dang, H., Tang, L.Y., Wang, X., et al., 2018. Non-proteolytic ubiquitin modification of PPARγ by Smurf1 protects the liver from steatosis. PLoS Biology 16(12):e3000091.

[14] Smyth, G.K., 2005. Limma: linear models for microarray data. In: Gentleman, R., Carey, V.J., Huber, W., Irizarry, R.A., Dudoit, S. (Eds.), Bioinformatics and computational biology solutions using R and bioconductor. Statistics for biology and health. New York, NY: Springer.

[15] Wu, D., Smyth, G.K., 2012. Camera: a competitive gene set test accounting for inter-gene correlation. Nucleic Acids Research 40(17):e133.

[16] Benjamini, Y., Hochberg, Y., 1995. Controlling the false discovery rate: a practical and powerful approach to multiple testing. Journal of the Royal Statistical Society: Series B 57(1):289–300.

[17] Chen, E.Y., Tan, C.M., Kou, Y., Duan, Q., Wang, Z., Meirelles, G.V., et al., 2013. Enrichr: interactive and collaborative HTML5 gene list enrichment analysis tool. BMC Bioinformatics 14:128.

[18] Kuleshov, M.V., Jones, M.R., Rouillard, A.D., Fernandez, N.F., Duan, Q., Wang, Z., et al., 2016. Enrichr: a comprehensive gene set enrichment analysis web server 2016 update. Nucleic Acids Research 44(W1):W90–W97.

[19] Blaise, B.J., Giacomotto, J., Elena, B., Dumas, M.E., Toulhoat, P., Ségalat, L., et al., 2007. Metabotyping of Caenorhabditis elegans reveals latent phenotypes. Proceedings of the National Academy of Sciences of the U S A 104(50):19808–19812.

[20] Dumas, M.E., Barton, R.H., Toye, A., Cloarec, O., Blancher, C., Rothwell, A., et al., 2006. Metabolic profiling reveals a contribution of gut microbiota to fatty liver phenotype in insulin-resistant mice. Proceedings of the National Academy of Sciences of the United States of America 103(33):12511–12516.

[21] Marino, A., Menghini, R., Fabrizi, M., Casagrande, V., Mavilio, M., Stoehr, R., et al., 2014. ITCH deficiency protects from diet-induced obesity. Diabetes 63(2):550–561.

[22] Fang, D., Elly, C., Gao, B., Fang, N., Altman, Y., Joazeiro, C., et al., 2002. Dysregulation of T lymphocyte function in itchy mice: a role for Itch in TH2 differentiation. Nature Immunology 3(3):281–287.

[23] Zhang, H., Xing, L., 2013. Ubiquitin e3 ligase itch negatively regulates osteoblast differentiation from mesenchymal progenitor cells. Stem Cells 31(8):1574–1583.

[24] Liu, J., Li, X., Zhang, H., Gu, R., Wang, Z., Gao, Z., et al., 2017. Ubiquitin E3 ligase Itch negatively regulates osteoblast function by promoting proteasome degradation of osteogenic proteins. Bone Joint Res 6(3):154–161.

[25] Kirsch, R., Clarkson, V., Shephard, E.G., Marais, D.A., Jaffer, M.A., Woodburne, V.E., et al., 2003. Rodent nutritional model of non-alcoholic steatohepatitis: species, strain and sex difference studies. Journal of Gastroenterology and Hepatology 18(11):1272–1282.

[26] Lee, Y.H., Kim, S.H., Kim, S.N., Kwon, H.J., Kim, J.D., Oh, J.Y., et al., 2016. Sex-specific metabolic interactions between liver and adipose tissue in MCD diet-induced non-alcoholic fatty liver disease. Oncotarget 7(30):46959–46971.

[27] Wu, C.W., Chu, E.S., Lam, C.N., Cheng, A.S., Lee, C.W., Wong, V.W., et al., 2010. PPARgamma is essential for protection against nonalcoholic steatohepatitis. Gene Therapy 17(6):790–798.

[28] Nan, Y., Wang, R., Zhao, S., Han, F., Wu, W.J., Kong, L., et al., 2010. Heme oxygenase-1 prevents non-alcoholic steatohepatitis through suppressing hepatocyte apoptosis in mice. Lipids in Health and Disease 9:124.

[29] Li, Q., Liu, B., Breitkopf-Heinlein, K., Weng, H., Jiang, Q., Dong, P., et al., 2019. Adenovirus-mediated overexpression of bone morphogenetic protein-9 promotes methionine choline deficiency-induced non-alcoholic steatohepatitis in non-obese mice. Molecular Medicine Reports 20(3):2743–2753.

[30] He, Y., Rodrigues, R.M., Wang, X., Seo, W., Ma, J., Hwang, S., et al., 2021. Neutrophil-to-hepatocyte communication via LDLR-dependent miR-223-enriched extracellular vesicle transfer ameliorates nonalcoholic steatohepatitis. Journal of Clinical Investigation 131(3):e141513.

[31] Casagrande, V., Mauriello, A., Bischetti, S., Mavilio, M., Federici, M., Menghini, R., 2017. Hepatocyte specific TIMP3 expression prevents diet dependent fatty liver disease and hepatocellular carcinoma. Scientific Reports 7(1):6747.

[32] Stöhr, R., Mavilio, M., Marino, A., Casagrande, V., Kappel, B., Möllmann, J., et al., 2015. ITCH modulates SIRT6 and SREBP2 to influence lipid metabolism and atherosclerosis in ApoE null mice. Scientific Reports 5:9023.

[33] Aki, D., Zhang, W., Liu, Y.C., 2015. The E3 ligase Itch in immune regulation and beyond. Immunological Reviews 266(1):6–26.

[34] Venuprasad, K., Zeng, M., Baughan, S.L., Massoumi, R., 2015. Multifaceted role of the ubiquitin ligase Itch in immune regulation. Immunology & Cell Biology 93(5):452–460.

[35] Bedossa, P., Tordjman, J., Aron-Wisnewsky, J., Poitou, C., Oppert, J.M., Torcivia, A., et al., 2017. Systematic review of bariatric surgery liver biopsies clarifies the natural history of liver disease in patients with severe obesity. Gut 66(9):1688–1696.

[36] Rappa, F., Greco, A., Podrini, C., Cappello, F., Foti, M., Bourgoin, L., et al., 2013. Immunopositivity for histone macroH2A1 isoforms marks steatosis-associated hepatocellular carcinoma. PLoS One 8(1):e54458.

[37] Lu, S.C., Mato, J.M., 2012. S-adenosylmethionine in liver health, injury, and cancer. Physiological Reviews 92(4):1515–1542.

[38] Park, E.J., Lee, J.H., Yu, G.Y., He, G., Ali, S.R., Holzer, R.G., et al., 2010. Dietary and genetic obesity promote liver inflammation and tumorigenesis by enhancing IL-6 and TNF expression. Cell 140(2):197–208.

[39] Field, N.S., Moser, E.K., Oliver, P.M.J., 2020. Itch regulation of innate and adaptive immune responses in mice and humans. Leukoc Biol 108(1):353–362.

[40] Masoodi, M., Gastaldelli, A., Hyötyläinen, T., Arretxe, E., Alonso, C., Gaggini, M., et al., 2021. Metabolomics and lipidomics in NAFLD: biomarkers and non-invasive diagnostic tests. Nature Reviews Gastroenterology & Hepatology. https://doi.org/10.1038/s41575-021-00502-9.

[41] Teufel, A., Itzel, T., Erhart, W., Brosch, M., Wang, X.Y., Kim, Y.O., et al., 2016. Comparison of gene expression patterns between mouse models of nonalcoholic fatty liver disease and liver tissues from patients. Gastroenterology 151(3):513–525.e0.

[42] Abdul Rahim, M.B.H., Chilloux, J., Martinez-Gili, L., Neves, A.L., Myridakis, A., Gooderham, N., et al., 2019. Diet-induced metabolic changes of the human gut microbiome: importance of short-chain fatty acids, methylamines and indoles. Acta Diabetologica 56(5):493–500.

[43] Mayneris-Perxachs, J., Cardellini, M., Hoyles, L., Latorre, J., Davato, F., Moreno-Navarrete, J.M., et al., 2021. Iron status influences non-alcoholic fatty liver disease in obesity through the gut microbiome. Microbiome 9(1):104.

[44] von Schönfels, W., Patsenker, E., Fahrner, R., Itzel, T., Hinrichsen, H., Brosch, M., et al., 2015. Metabolomic tissue signature in human non-alcoholic fatty liver disease identifies protective candidate metabolites. Liver International 35(1):207–214.

[45] Lake, A.D., Novak, P., Shipkova, P., Aranibar, N., Robertson, D.G., Reily, M.D., et al., 2015. Branched chain amino acid metabolism profiles in progressive human nonalcoholic fatty liver disease. Amino Acids 47(3):603–615.

[46] White, P.J., McGarrah, R.W., Herman, M.A., Bain, J.R., Shah, S.H., Newgard, C.B., 2021. Insulin action, type 2 diabetes, and branched-chain amino acids: a two-way street. Molecular Metabolism 52:101261.

[47] Bernassola, F., Chillemi, G., Melino, G., 2019. HECT-type E3 ubiquitin ligases in cancer. Trends in biochemical sciences 44(12):1057–1075.

[48] Melino, G., Cecconi, F., Pelicci, P.G., Mak, T.W., Bernassola, F., 2019. Emerging roles of HECT-type E3 ubiquitin ligases in autophagy regulation. Mol Oncol 13(10):2033—2048.
[49] Karusheva, Y., Koessler, T., Strassburger, K., Markgraf, D., Mastrototaro, L., Jelenik, T., et al., 2019. Short-term dietary reduction of branched-chain amino acids reduces meal-induced insulin secretion and modifies microbiome composition in type 2 diabetes: a randomised controlled crossover trial. American Journal of Clinical Nutrition 110(5):1098—1107.
[50] White, P.J., Lapworth, A.L., An, J., Wang, L., McGarrah, R.W., Stevens, R.D., et al., 2016. Branched-chain amino acid restriction in Zucker-fatty rats improves muscle insulin sensitivity by enhancing efficiency of fatty acid oxidation and acyl-glycine export. Molecular Metabolism 5(7):538—551.
[51] Lee, J., Vijayakumar, A., White, P.J., Xu, Y., Ilkayeva, O., Lynch, C.J., et al., 2021. BCAA supplementation in mice with diet-induced obesity alters the metabolome without impairing glucose homeostasis. Endocrinology 162(7):bqab062.
[52] Maida, A., Chan, J.S.K., Sjøberg, K.A., Zota, A., Schmoll, D., Kiens, B., et al., 2017. Repletion of branched chain amino acids reverses mTORC1 signaling but not improved metabolism during dietary protein dilution. Molecular Metabolism 6(8):873—881.
[53] Buzzetti, E., Pinzani, M., Tsochatzis, E.A., 2016. The multiple-hit pathogenesis of non-alcoholic fatty liver disease (NAFLD). Metabolism 65(8):1038—1048.
[54] Kleine-Eggebrecht, N., Staufner, C., Kathemann, S., Elgizouli, M., Kopajtich, R., Prokisch, H., et al., 2019. Mutation in ITCH gene can cause syndromic multisystem Autoimmune disease with acute liver failure. Pediatrics 143(2): e20181554.
[55] Lohr, N.J., Molleston, J.P., Strauss, K.A., Torres-Martinez, W., Sherman, E.A., Squires, R.H., et al., 2010. Human ITCH E3 ubiquitin ligase deficiency causes syndromic multisystem autoimmune disease. The American Journal of Human Genetics 86(3):447—453.
[56] Neinast, M., Murashige, D., Arany, Z., 2019. Branched chain amino acids. Annual Review of Physiology 81:139—164.
[57] Neinast, M.D., Jang, C., Hui, S., Murashige, D.S., Chu, Q., Morscher, R.J., et al., 2019. Quantitative analysis of the whole-body metabolic fate of branched-chain amino acids. Cell Metabolism 29(2):417—429.e4.
[58] Liu, S., Li, L., Lou, P., Zhao, M., Wang, Y., Tang, M., et al., 2021. Elevated branched-chain α-keto acids exacerbate macrophage oxidative stress and chronic inflammatory damage in type 2 diabetes mellitus. Free Radical Biology and Medicine 175:141—154.
[59] Papathanassiu, A.E., Ko, J.H., Imprialou, M., Bagnati, M., Srivastava, P.K., Vu, H.A., et al., 2017. BCAT1 controls metabolic reprogramming in activated human macrophages and is associated with inflammatory diseases. Nature Communications 8:16040.
[60] Hooper, C., Puttamadappa, S.S., Loring, Z., Shekhtman, A., Bakowska, J.C., 2010. Spartin activates atrophin-1-interacting protein 4 (AIP4) E3 ubiquitin ligase and promotes ubiquitination of adipophilin on lipid droplets. BMC Biology 8:72.
[61] Griffin, J.D., Bejarano, E., Wang, X.D., Greenberg, A.S., 2021. Integrated action of autophagy and adipose tissue triglyceride lipase ameliorates diet-induced hepatic steatosis in liver-specific PLIN2 knockout mice. Cells 10(5):1016.
[62] Nocetti, D., Espinosa, A., Pino-De la Fuente, F., Sacristán, C., Bucarey, J.L., Ruiz, P., et al., 2020. Lipid droplets are both highly oxidized and Plin2-covered in hepatocytes of diet-induced obese mice. Applied Physiology Nutrition and Metabolism 45(12):1368—1376.
[63] Jin, Y., Tan, Y., Chen, L., Liu, Y., Ren, Z., 2018. Reactive oxygen species induces lipid droplet accumulation in HepG2 cells by increasing perilipin 2 expression. International Journal of Molecular Sciences 19(11):3445.
[64] Conte, M., Franceschi, C., Sandri, M., Salvioli, S., 2016. Perilipin 2 and age-related metabolic diseases: a new perspective. Trends in Endocrinology and Metabolism 27(12):893—903.
[65] Robichaud, S., Fairman, G., Vijithakumar, V., Mak, E., Cook, D.P., Pelletier, A.R., et al., 2021. Identification of novel lipid droplet factors that regulate lipophagy and cholesterol efflux in macrophage foam cells. Autophagy 26:1—19.
[66] Filali-Mouncef, Y., Hunter, C., Roccio, F., Zagkou, S., Dupont, N., Primard, C., et al., 2021. The menage a trois of autophagy, lipid droplets and liver disease. Autophagy 2:1—24.
[67] Li, F., Ma, K., Sun, M., Shi, S., 2018. Identification of the tumor-suppressive function of circular RNA ITCH in glioma cells through sponging miR-214 and promoting linear ITCH expression. Am J Transl Res 10(5):1373—1386.
[68] Li, F., Zhang, L., Li, W., Deng, J., Zheng, J., An, M., et al., 2015. Circular RNA ITCH has inhibitory effect on ESCC by suppressing the Wnt/beta-catenin pathway. Oncotarget 6(8):6001—6013.
[69] Li, Y., Ge, Y.Z., Xu, L., Jia, R., 2020. Circular RNA ITCH: a novel tumor suppressor in multiple cancers. Life Sciences 254:117176.
[70] Yang, B., Zhao, J., Huo, T., Zhang, M., Wu, X., 2020. Effects of CircRNA-ITCH on proliferation and apoptosis of hepatocellular carcinoma cells through inhibiting Wnt/beta-catenin signaling pathway. J BUON 25(3):1368—1374.
[71] Wu, M., Deng, X., Zhong, Y., Hu, L., Zhang, X., Liang, Y., et al., 2020. MafF is regulated via the circ-ITCH/miR-224-5p Axis and acts as a tumor suppressor in hepatocellular carcinoma. Oncology Research Featuring Preclinical and Clinical Cancer Therapeutics 28(3):299—309.
[72] Guo, W., Zhang, J., Zhang, D., Cao, S., Li, G., Zhang, S., et al., 2017. Polymorphisms and expression pattern of circular RNA circ-ITCH contributes to the carcinogenesis of hepatocellular carcinoma. Oncotarget 8(29):48169—48177.

